for the recorded ground motion. The record of ground motion from a recording station located on the side or bottom of a valley will be influenced by the shape of the valley. These effects have not been considered in the present study.

(iv) The recorded accelerogram is influenced by closeness of the causative fault, its size, pattern of slip distribution, form of source time function, rise time, rupture velocity and model of rupture propagation (unilateral, bilateral, circular, etc.). The size of the fault can be estimated. However, other properties of the source are not known in advance.

(v) As stated earlier the objective of the present study is to determine the usefulness of a method of synthetic seismogram generation proposed herein. The synthetic accelerograms generated in the present study show a satisfactory match with the observed ones in a number of sites, demonstrating the usefulness of the method of synthetic seismogram generation.

1. Abrahamson, N. P., Somerville, P. G. and Cornell, C. A., Goodness of fit for numerical strong motion simulations and uncertainty in numerical strong motion simulations predictions. Proceedings of the 4th US National Conference on Earthquake Engineering, Palm Springs, California, 1990, vol. 1, pp. 317–326.
2. Makaris, D. I., Stavrakakis, G. N. and Drakopoulos, J. C., Expected ground motion at a site based on hypothetical fault models. *Earthquake Engineering*, Tenth World Conference, Balkema, Rotterdam, 1992, vol. 2, pp. 703–708.
3. Barker, J. S., Somerville, P. G. and McLaren, J. P., Modelling of ground motion attenuation in Eastern North America. Electric Power Research Institute Report NP-5577, 1988, p. 414.
4. Wald, D. J., Helmberger, D. V. and Heaton, T. H., Rupture model of the 1989 Loma Prieta earthquake from the inversion of strong motion and broadband and teleseismic data. *Bull. Seismol. Soc. Am.*, 1991, **81**, 1540–1572.
5. Zeng, Y., Aki, K. and Teng, L., Source inversion of the 1987 Whittier narrows earthquake, California, using the isochron method. *Bull. Seismol. Soc. Am.*, 1993, **83**, 358–377.
6. Zeng, Y., Aki, K. and Teng, L., Mapping of the high frequency source radiation for the Loma Prieta earthquake, California. *J. Geophys. Res.*, 1993, **98**, 11981–11993.
7. Somerville, P., Engineering applications of strong ground motion simulation. *Tectonophysics*, 1993, **218**, 195–219.
8. Zeng, Y., Anderson, J. G. and Yu, G., A composite source model for computing realistic synthetic strong motions. *Geophys. Res. Lett.*, 1994, **21**, 725–728.
9. Zeng, Y., Anderson, J. G. and Su, F., Source and path effects in realistic strong ground motion simulation. *Seism. Res. Lett.*, Abstract, 1994, **65**, 36.
10. Khattri, K. N., Yu, G., Anderson, J. G., Brune, J. N. and Zeng, Y., Seismic hazard estimation using modeling of earthquake strong ground motions: A brief analysis of 1991 Uttarkashi earthquake, Himalaya and prognostication for a great earthquake in the region. *Curr. Sci.*, 1994, **67**, 343–353.
11. Yu, G., Khattri, K. N., Anderson, J. G., Brune, J. N. and Zeng, Y., Strong ground motion from the Uttarkashi, Himalaya, India, earthquake: Comparison of observations with synthetics using the composite source model. *Bull. Seismol. Soc. Am.*, 1995, **85**, 31–50.
12. Kumar, D., Khattri, K. N., Teotia, S. S. and Rai, S. S., Modeling of accelerograms of two Himalayan earthquakes using a novel semi-empirical method and estimation of accelerograms for a Hypothetical great earthquake in the Himalaya. *Curr. Sci.*, 1999, **76**, 819–830.
13. Khattri, K. N., Zeng, Y., Anderson, J. G. and Brune, J., Inversion of strong motion waveforms for source slip function of 1991 Uttarkashi earthquake, Himalaya. *J. Himalayan Geol.*, 1994, **5**, 163–191.
14. Kasahara, K., *Earthquake Mechanics*, Cambridge University Press, 1981.
15. Aki, K. and Richards, P. G., *Quantitative Seismology: Theory and Methods*, W. H. Freeman and Company, San Francisco, 1980, vols 1 and 2.
16. Boore, D. M., The prediction of strong ground motion. In *Strong Ground Motion Seismology* (eds Erdik, M. and Toksoz, M. N.), NATO Advanced Studies Institute Series, D. Reidel Publishing Company, Dordrecht, 1987, pp. 109–141.
17. Boore, D. M., Stochastic simulation of high frequency ground motions based on seismological models of the radiated spectra. *Bull. Seismol. Soc. Am.*, 1983, **73**, 1865–1894.
18. Valdiya, K. S., Tectonics and evolution of the central sector of the Himalaya. *Philos. Trans. R. Soc. London*, 1988, **4326**, 151–175.
19. Seeber, L. and Armbruster, J. G., Great detachment earthquakes along the Himalayan arc and long term forecasting. In *Earthquake Prediction: An International Review*, Maurice Ewing Series, 4, American Geophysical Union, Washington DC, 1981, pp. 259–277.
20. Khattri, K. N., Local seismic investigation in the Garhwal-Kumaon Himalayas. *Mem. Geol. Soc. India*, 1992, **23**, 45–66.
21. Ben-Menahem, A. and Singh, S. J., *Seismic Waves and Sources*, Springer-Verlag, New York, 1981, p. 1108.
22. Chandrasekaran, A. R. and Das, J. D., Strong motion records from Uttarkashi earthquake. *Mem. Geol. Soc. India*, 1995, 133–147.
23. IMD, Chamoli earthquake of 29 March 1999 and its aftershocks. India Meteorological Department, Government of India, Seismology No. 2/2000, 2000, p. 70.

ACKNOWLEDGEMENT. We thank the Director, CBRI, Roorkee and Head, Department of Earth Sciences, IIT Roorkee for support.

Received 22 April 2004; revised accepted 16 December 2004

The tsunami of the great Sumatra earthquake of *M* 9.0 on 26 December 2004 – Impact on the east coast of India

R. K. Chadha[1,*], G. Latha[2], Harry Yeh[3], Curt Peterson[4] and Toshitama Katada[5]

[1]National Geophysical Research Institute, Hyderabad 500 007, India
[2]National Institute of Ocean Technology, Chennai 601 302, India
[3]Department of Civil Engineering, Oregon State University, Corvallis, Oregon 97336-4501, USA
[4]College of Liberal Arts and Science, Portland State University, Portland, Oregon 97207, USA
[5]Gunma University 1-5-1, Tenjincho, Kiryu, Gunma, 376-8515, Japan

An earthquake of magnitude 9.0 occurred off the coast of Sumatra on 26 December 2004 at 00 : 58 : 50 (UTC)/ 06 : 28 : 50 AM (IST). The epicentre of the earthquake was located at 3.29°N and 95.94°E. The focal depth of

*For correspondence. (e-mail: chadha@ngri.res.in)

the earthquake was 30 km. This earthquake generated huge tsunami waves which devastated the Andaman and Nicobar Islands, east coast of India, south Kerala in India and several other countries like Sri Lanka, Indonesia, Thailand and Somalia in the Indian Ocean. The tsunami claimed more than 250,000 human lives in these countries. The aftershocks of this earthquake, numbering more than 250 in the magnitude range $5 \leq M < 7.3$, were located for a length of 1300 km from Sumatra in the south to the Andaman and Nicobar islands in the north, till 30 January 2005. A tsunami run-up survey was conducted immediately after the event to study tsunami damages, inundation areas and to obtain estimates of tsunami heights from perishable evidences like watermarks on houses and ocean debris transported inland. This communication presents results on tsunami heights at different locations along the coastal areas of Tamil Nadu.

ON 26 December 2004, an earthquake of M 9.0 shook the entire east coast of India and Andaman and Nicobar Islands at 06 : 29 h (IST). Centred off the coast of Sumatra in the Indian Ocean, the earthquake caused extensive damage in the Andaman and Nicobar Island regions of India and was felt strongly all along the east coast of India from Srikakulam in Andhra Pradesh (AP) to Nagapattinam in Tamil Nadu (TN). Some of the houses in the coastal belt of AP developed cracks. The earthquake set-off huge tsunami, which travelled throughout the world oceans, severely affecting several countries in the Indian Ocean. Most severely affected countries in descending order are Indonesia, Thailand, Sri Lanka, India and Somalia. The Nicobar Islands, situated within 500 km from the epicentre of the earthquake were the first to be devastated, followed by the Andaman region of India. The tsunami travelled a distance of more than 2000 km in the Indian Ocean and severely affected the east coast of India from Srikakulam in AP to Kanyakumari in TN. Southern parts of coastal Kerala also suffered severe damage due to wrap-up effects of the tsunami propagation. Figure 1 shows the travel time of the tsunami in the Indian Ocean. It is seen that the east coast of India was affected by the tsunami after more than 2 h of the main earthquake at 06 : 29 h (IST). Damage to life and property due to the tsunami was most severe from Chennai to south of Nagapattinam along the TN coast, where more than 7800 people died. Wherever the shoreline rises steeply or was protected by mangroves, the damage was less pronounced; but all along the shallow beaches, the damage was severe. This communication presents a joint report by Indian scientists and an international survey team that visited the TN coast immediately after the tsunami, to estimate the run-up heights and inundation areas, and assess the damages.

A field survey was taken up by the National Geophysical Research Institute (NGRI), Hyderabad in AP and TN immediately after the Sumatra earthquake, to study the effects along the east coast of India. Some scientists from NGRI and National Institute of Ocean Technology (NIOT), Chennai joined the international tsunami survey team of Earthquake Engineering Research Institute (EERI), USA from 7 to 11 January 2005. The objective of the survey was to measure tsunami run-up heights, map the inundation areas and assess the damage caused by the tsunami along the TN coast. Run-up heights are the maximum vertical distance reached by tsunami, measured relative to the mean sea level. Estimation of run-up heights was done based on physical evidence like the watermarks or debris carried inland by the tsunami. During the survey, information was also gathered from eyewitnesses and newspapers. This information is subject to errors of the order of few tens of centimetres and generally within 10–15% error of the measured data. The surveys were carried out with a bubble-level transit mounted on a tripod and extendable stadia rod and also a hand-held level, GPS for locations of indicators on maps and at some places based on the location of samples of sediments carried inland.

In AP, 106 people were confirmed dead and seven missing. The most affected districts were Krishna and Prakasam, recording 27 and 35 deaths respectively. Other affected districts were Guntur, Nellore, West Godavari, East Godavari and Visakhapatnam. The tsunami is reported to have encroached 500 m to 2 km at various places owing to the flatness of several beaches. Tide-gauge recorder at Visakhapatnam port in AP showed tsunami heights to be about 1.4 m at 09 : 05 h. Although eyewitnesses reported tsunami heights up to 5 m, based on our surveys, we estimate the maximum tsunami height to be 2.5 m along the AP coastline, with higher splashes at a few places. However, there was a general agreement amongst people that four waves hit the coast, in which the second wave was the strongest and claimed most lives. Several people reported receding of the sea up to 500 m prior to the arrival of tsunami in the region.

A detailed tsunami run-up survey was carried out along a 350 km long stretch of the shoreline in TN from Pulicat (13.3° lat.) in the north to Vedaranniyam (10.3° lat.) in the south. Shore-normal inundation profiles were studied at 11 locations to estimate the run-up heights of the tsunami. Survey localities were selected on the basis of reports of maximum damage and loss of lives. Profiles within the survey localities were selected on the basis of representative high-watermarks and line-of-sight traverses to beach swash zones. High watermarks were measured from the highest elevations of several different indicators. These indicators include (i) mud lines on standing structures, i.e. maximum still-water elevation, (ii) physical damage to standing structures, i.e. maximum surge elevation and (iii) flotsam debris on tree branches, roofs and ground slopes, i.e. maximum splash elevations and/or maximum inundation distances[1].

Maximum still-water elevations were preferentially taken from interior-wall mudline, which should minimize effects from turbulent flow around structures. Exterior-wall mudlines were used where horizontal mudlines could be correlated between buildings. The vertical distance between the

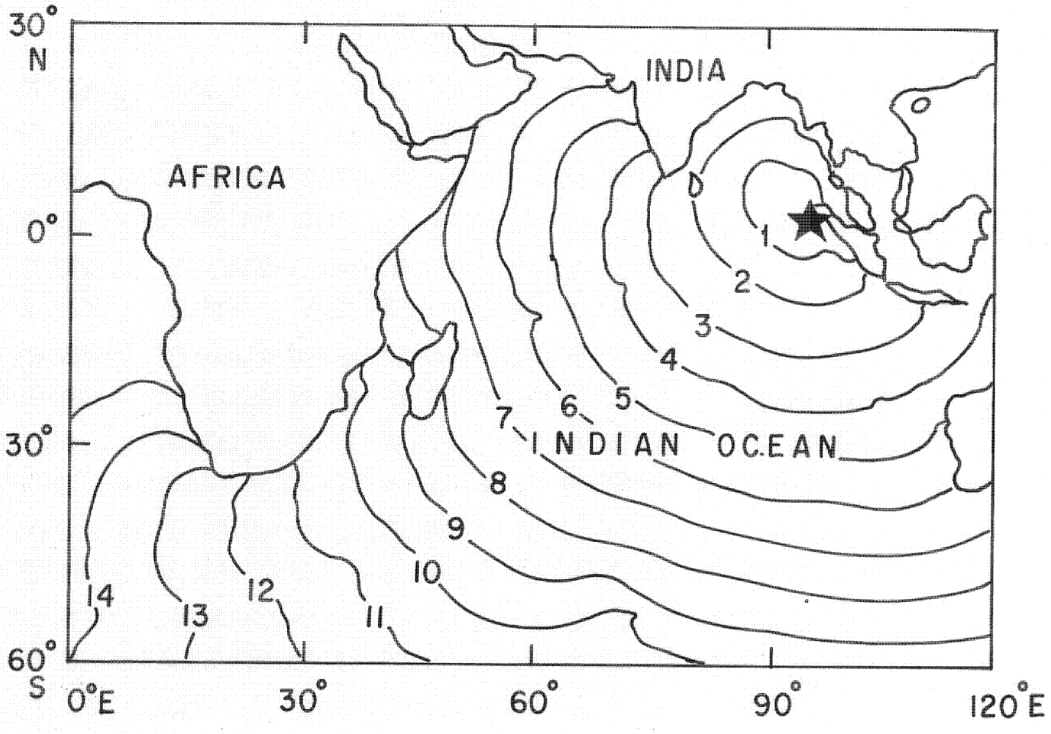

Figure 1. Travel-time of tsunami waves in the Indian Ocean. Contour interval is 1 h. Star shows epicentre of the Sumatra earthquake of *M* 9.0 on 26 December 2004 (Source: NOAA).

highest horizontal mudline and ground elevation, i.e. tripod footings surface was measured to the nearest centimetre with a tape. Maximum surge elevations were estimated from features reflecting apparent large debris damage at elevations above the mud lines. These features included displaced roof tiles, broken masonry, fresh gouges in plaster and heavy woody debris left in broken or bent tree branches. Maximum splash elevations were established from light flotsam hanging in limbs of standing vegetation and/or draped on standing structures such as railings and roofs. Horizontal sighting distances were generally less than 100 m between level and stadia rod. Elevations were measured to the nearest centimetre. Total profile errors of ± 0.1 m are assumed for the single-sighting, single-direction, levelling surveys. End points of the profiles were approximately located by 12-channel GPS using the WGS84 datum. Three levels of flow competence were established from maximum landward transport of gravel, sand and flotsam debris. The gravel-size material included large (> 2 cm diameter) shells, brick and mortar fragments and road gravel. General lack of gravel source material likely precluded high flow competence in some areas. Beach sand (0.06 to 2 mm grain diameter) was present in almost all the profiles. Maximum inundation positions were generally evident from semi-continuous lines of debris that crossed streets, vacant lots, fields and wetland surfaces. Large inundation distances in some locations were related to localized flow through dune-ridge gaps or tidal inlets. Overland flow direction was measured from several different features. These features included vegetation, flop-overs and debris shields wrapped around trunks and sand ripples and linear-scours[2].

Figure 2 shows the tsunami run-up heights estimated for 11 localities along the TN coast from Pulicat in the north to Vedaranniyam in the south. The tsunami height varies between 2.5 and 5.2 m in these regions, after applying tidal corrections from tide tables published by Survey of India. Maximum surge elevations were also measured and were found to vary between 3.8 and 6.0 m (mean tidal level).

Three zones of flow competence were established from the maximum transport distances of gravel, sand and flotsam in the 11 profiles surveyed. Gravel transport ranged from 30 to 60 m distance from the swash zone in Pattinapakam, Periakalapet, Devanaampatnam and Tarangambadi profiles. The gravel-size clasts were largely derived from tsunami-damaged brick walls, foundations and roofing tiles in the region. Maximum sand transport ranged from 90 to 430 m distance from the swash zone in most of the profiles (Table 1). Beach width in most of the profiles varies between 30 and 50 m, except at Parangipettai and Nagapattinam, where it was about 300 m. With the exception of these profiles, the average sand transport distance is about 100 m beyond the beach backshore. Tsunami sand deposits ranged from coarse upper (700–1000 μm) to very fine upper (88–125 μm) in grain size, based on comparisons with grain-size cards. Sand sheet thickness ranged from several tens of centimetres near the beach backshore to 1 cm thickness at the distal

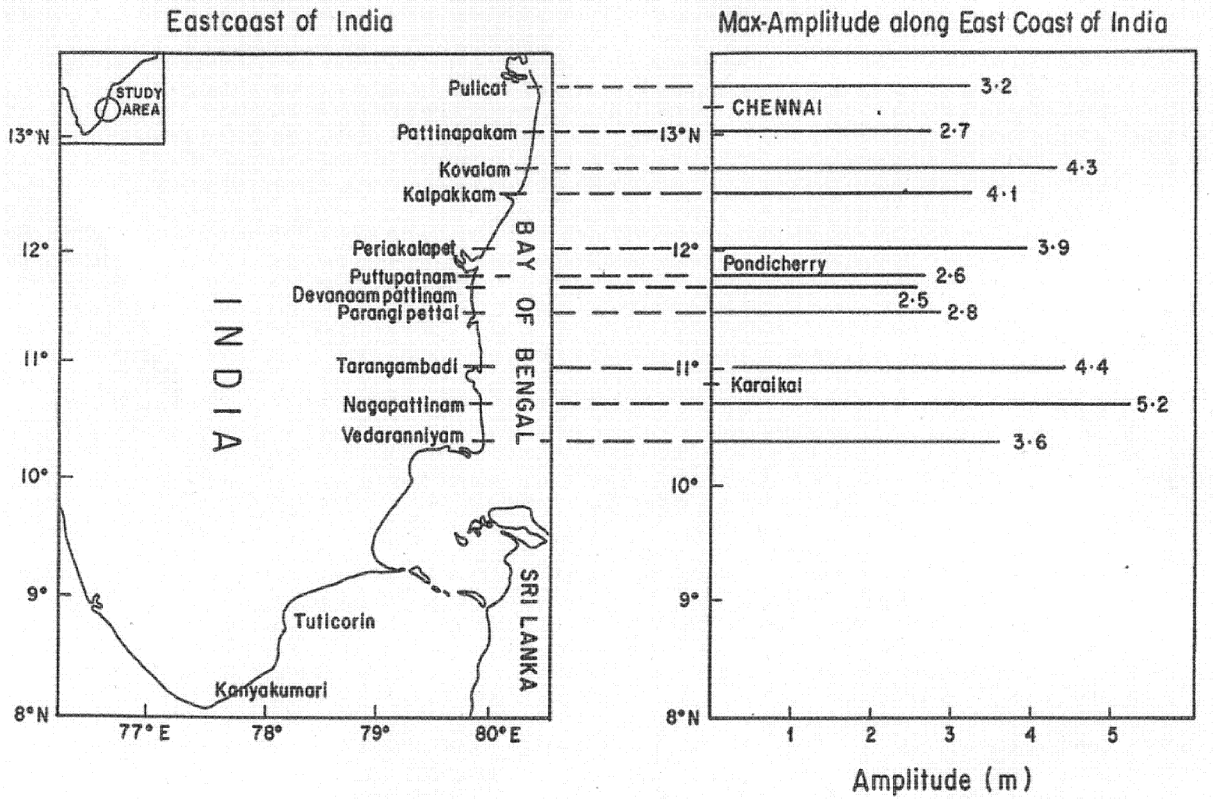

Figure 2. Tsunami run-up heights at different locations along the east coast of Tamil Nadu. Numbers are tsunami heights in metres.

Table 1. Details of tsunami run-up survey along the coast of Tamil Nadu

Location	Latitude °N/ longitude °E	Run-up elevation (m)	Lateral inundation (m)	Max. sand distance (m)
Pulicat	13°23.040′ 80°19.984′	3.2	160	90
Pattinapakam	13°01.263′ 80°16.722′	2.7	145	120
Kovalam	12°47.455′ 80°15.003′	4.3	180	120
Kalpakkam	12°30.378′ 80°09.688′	4.1	360	190
Periakalapet	12°01.544′ 79°51.888′	3.9	170	130
Puttupatnam	11°51.618′ 79°48.926′	2.6	–	–
Devanaampatnam	11°44.576′ 79°47.230′	2.5	340	180
Parangipettai	11°30.965′ 79°45.947′	2.8	700	400
Tarangambadi	11°01.620′ 79°51.350′	4.4	400	150
Nagapattinam	10°45.785′ 79°50.928′	5.2	800	430
Vedaranniyam	10°23.597′ 79°52.014′	3.6	–	–

end of sand transport. With increasing distance landward, the mean grain size of the sand sheets appeared to decrease. The graded sequence from coarse to fine upwards in each of 2–3 sand layers was observed at the 80 m position at Devanaampatnam. Maximum inundation distances along the profiles were established on the basis of most landward

distribution of flotsam in debris lines or of anomalous articles, e.g. clothing mats, fishing floats, etc. Maximum inundation ranged between 140 and 800 m from the swash zone. Based on local topography, flow direction indicators and the orientation of debris lines, it was apparent that maximum landward inundation occurred by lateral flow at Pulicat, Devanaampatnam, Parangipettai and Taramgambadi. Lateral flows filled interdune-ridge valleys that were landward of shore-parallel dune-ridges at Devanaampatnam and Parangipettai. The interdune-ridge valleys at the landward ends of these two profiles were connected to tidal inlet channels. Lateral flow also filled shallow valleys in Pulicat and Tarangambadi, where breaches in shore-parallel dune-ridges allowed the tsunami to inundate back-ridge areas.

Flow features were recorded in most of the profiles that include vegetation flop-over, orientated beams, debris shields around tree trunks and sand ripples. The mean bearing of measured flow direction was observed to be 250° from true north. Data suggest an oblique angle of tsunami wave attack, particularly in profiles between 11.5 and 12° lat where the shoreline trends NNE. The tsunami wave attack was observed to be of the order of 30–40° from the shore normal in the study area.

From our surveys, we infer the following: (i) The tsunami run-up heights along the east coast of India in TN vary between 2.5 and 5.2 m. (ii) Loss of life and property was reported in the first 100 m from the shore, where several settlements were washed away. (iii) Small differences in local run-up and coastal topography resulted in large differences in tsunami inundation and associated loss of life and damage within the TN coastal areas. (iv) The combination of local high run-up, low topography and dense development apparently accounted for the large loss of life and property. The surge water elevations, together with surge water depths appear to be important parameters in tsunami hazard analysis. (v) Low valleys behind shore-parallel dune-ridges claimed several lives due to lateral flows from tidal inlets or from breaches in the dune ridge. (vi) Keeping in view the observations during our survey, a detailed study should be taken up to assess the inundation areas all along the eastern coast of India, to prepare inundation hazard maps to avoid loss of life and property.

1. UNESCO, *Post-Tsunami Survey Field Guide*, Intergovernmental Oceanographic Commission, UNESCO IOC/ITSU, 1997, p. 19.
2. Allen, J. R. L., *Sedimentary Structures: Their Character and Physical Basis*, Elsevier, Amsterdam, 1984, p. 663.

ACKNOWLEDGEMENTS. We thank the Directors of NGRI, Hyderabad and NIOT, Chennai and the US National Science Foundation through EERI for the support during the study. We acknowledge the support of Mr G. Raghuraman, NIOT, during fieldwork.

Received 8 February 2005; accepted 9 March 2005

Analysis of runoff pattern for all major basins of India derived using remote sensing data

Mohan Zade[1], S. S. Ray[1,*], S. Dutta[2] and S. Panigrahy[1]

[1]Agro-Ecology and Management Division, ARG/RESIPA, Space Applications Centre, Indian Space Research Organisation, Ahmedabad 380 015, India
[2]Department of Civil Engineering, Indian Institute of Technology, Guwahati 781 039, India

An attempt has been made to quantify and analyse intra- and inter-basin runoff potential for all basins of India using multi-date remote sensing data, curve number approach and normal rainfall data of 376 stations. Analysis showed that the highest runoff depth (1812 mm) was observed in the Brahmaputra basin (including Barak and other rivers) and the lowest (210 mm) in the Luni and rivers of Saurashtra basin. The Brahmputra basin, occupying only 8% of the geographical area of the country, provided around 19% of total runoff. In almost all basins, 90% runoff occurs during the five-month period starting from June. The runoff in the Brahmaputra, Narmada and Mahanadi basins responded well to rainfall, i.e. high runoff coefficient, whereas low runoff coefficient was found in the Cauvery basin.

THE status of water availability, particularly spatial and temporal pattern at the basin level is essential for regional planning and decision on water management. Runoff is an indication of availability of water. Thus *in situ* measurement of runoff is useful, however in most cases such measurements are not possible at the desired time and location as conventional techniques of runoff measurement are expensive, time-consuming and difficult. Therefore, rainfall–runoff models are commonly used for computing runoff. The model developed by the United States Department of Agriculture (USDA) Soil Conservation Society (SCS) known as curve number (CN) is popular among all rainfall–runoff models because of its simple mathematical relationships and low data requirement[1].

The CN represents the watershed coefficient, which is the combined hydrological effect of soil, land use, agricultural land treatment class, hydrological condition and antecedent soil moisture condition (AMC)[1]. Generally, the model is well suited for small watersheds of less than 4000 ha, as it requires details of soil physical properties, land use, conservation treatment and vegetation condition[2,3]. However, with increasing availability of finer spatial resolution information from space-based remote sensing data on vegetation, it is possible to use the SCS model for larger areas with better accuracy[4]. Gumbo *et al.*[5] found that the CN method worked well in GIS environment because of its relatively simple

*For correspondence. (e-mail: ssray@sac.isro.org)